Very High Cycle Fatigue Behavior and Thermographic Analysis of High Strength Steel

C. Shao, C. Bathias, Danièle Wagner, Hua Tao

Very High Cycle Fatigue Behavior and Thermographic Analysis of High Strength Steel

SHAO Chuang[1,2,3,a] ,Cloude BATHIAS[2,b], Danièle WAGNER[2], TAO Hua[1]

[1]School of Mechatronic Engineering, Northwestern Polytechnical University, Xi'an 710072, China

[2] LEEE, Université PARIS X, Ville d'avray, 92410, France

[3]Aircraft Strength Research Institute, Xi' an, 710065, China

[a]sch623@yahoo.cn, [b]cbathias@paris10.fr

Key Words: Very high cycle fatigue, High strength steel, Fish eye, Infrared imaging

Abstract. Very high cycle fatigue behavior of high strength steel, were investigated using ultrasonic fatigue testing equipment at 20 kHz up to 10^9cycles. S-N curves at room temperature with different stress ratio (R=0.01 and R=0.1) was determined. The experimental results show that fatigue strength decrease with increasing number of cycles between 10^5 and 10^9. SEM examination of fracture surface reveals that fatigue damage was governed by the formation of cracks, and subsurface crack initiation was in the very long life range. The results shown that the portions of life attributed to subsurface crack initiation between 10^7 and 10^9 cycles are 99%.

Introduction

The objective of this study is to determine the SN fatigue curve of a high strength steel supplied by one famous car manufacturing factory. It had been suggested to explore several levels of loading corresponding to fatigue lives between 10^5 to 10^9 cycles.

This paper shows the some results and some researches done to solve the problem of machining of specimens. Heating of the specimen is a difficulty and it is why we made a thermal recording of the specimen. It has been not possible to get some failures at 10^5 cycles because the heating dissipation at 20 kHz is very important, in low cycle fatigue.

Materials

Chemical composition. The steel is a low alloy and ultrahigh strength steel. The microstructure of this steel is martensite with residual austenite. The X-ray analysis of inclusions shows very small MnS inclusions and mixed inclusions (Al, Si, Mg, S, Mn) with larger diameters (Fig 1).

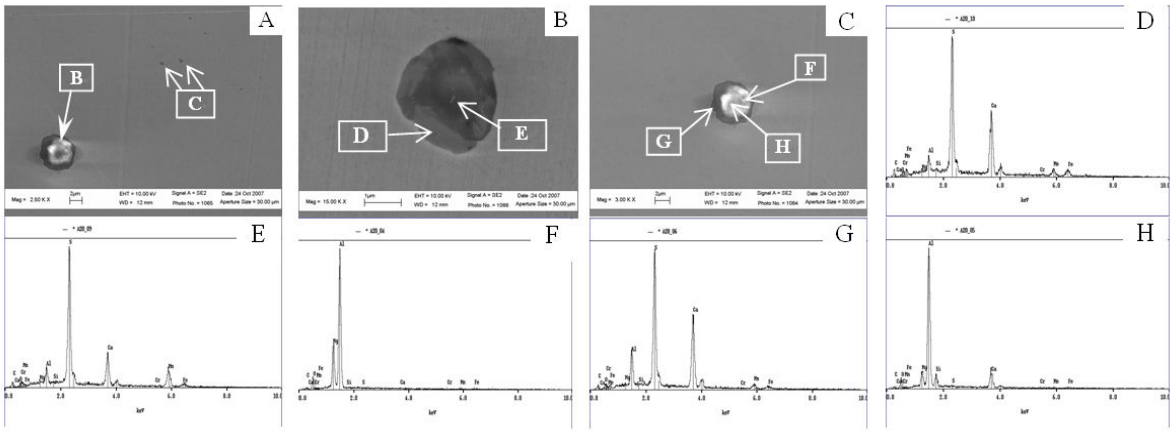

Fig.1 X-ray Analysis of Inclusions

Mechanical properties. UTS = 2000 MPa, Density = 7850 Kg/m3, Young's Modulus = 200 GPa, Standard Fatigue Limit (10^6 cycles) = 975 MPa.

All above are primal data. The hardness tests (Rochwell) of specimens after ultrasonic fatigue test have given HRC = 46 which correspond to a lower value of UTS (1527MPa).

Experimental

Mechanical test.

Description of the ultrasonic fatigue test device. Ultrasonic fatigue test machine is composed of power generator, vibration system and control unit. The basic structure and working theory of the machine is that: fatigue vibration system composed of converter, amplifier horn and specimen is a resonance system, the vibration of the resonance system is excited by the generator, the working produce of the system is controlled by control unit.

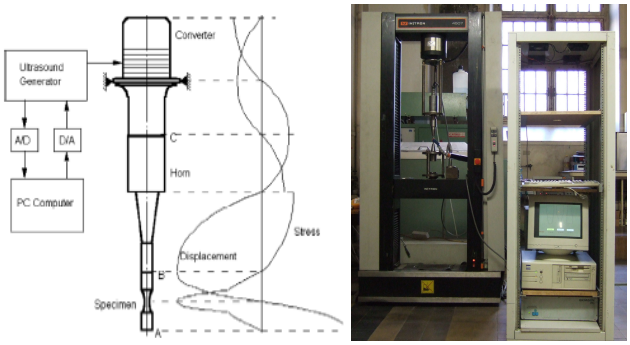

Fig.2 Piezoelectric Fatigue Machine for R=0.1 and R=0.01

The vibration system (Fig 2) for cyclic loading consists of a converter, amplifier and the specimen, under the excitation of a system of ultrasonic resonance. The amplifier and the specimen must have a length of resonance of 20 kHz.

As stated above, a ultrasonic fatigue test machine must include the following three common components:

a) A power generator that transform 50 or 60 Hz voltage signal into 20 kHz electrical sinusoidal signal.
b) A piezoelectric transducer excited by the power generator, which transforms the electrical signal into longitudinal ultrasonic waves and mechanical vibration of the same frequency.
c) An ultrasonic horn that amplifiers the vibration coming from the transducer to obtain the required strain amplitude in the middle section of the specimen. The converter, horn and specimen are from a mechanical vibration system. For different fatigue vibration machines, their vibration systems have different components and vibration modes.

Performed tests. In this work, the test was carried out with a stress ratio R=0.01 and R=0.1at several load levels. Compressed air like means of cooling of the specimens has been used to avoid an increase of the temperature (Fig 3).

Two horns were designed in order to carry the tests of this steel. The displacement is produced by the converter and amplified by horn. This last one amplifies the vibration and allows reaching to the specimen an important stress. The horn used for the tests is a horn which obtains an amplitude of displacement of 3µm to 20µm.

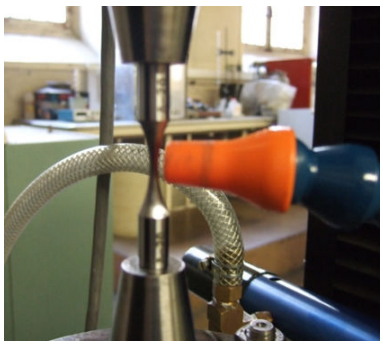

Figure 3. Specimen in the Machine and the Cooling Nozzle

The samples have been designed theoretically using the elastic theory of propagation of wave by the method of finite elements, calculating for a frequency of 20 kHz. The dimensions of the specimens (Fig 4), as well as the Stress-Displacement ratio is calculated using this method, and depends on the density and the modulus of elasticity of the steel. The Stress-Displacement ratio for the tested specimens is 25.8164 MPa/µm, according to the software 20 kHz in the fatigue machine system.

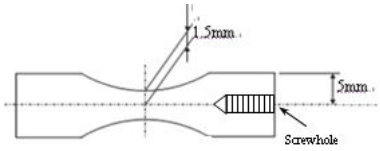

Fig 4. Sketch of Specimen Drawing

Thermal tests.

Description of the infrared camera device. In order to determine the temperature field on the test sample surface, a non-destructive measurement technique using an advanced high-speed, high-thermal camera was chosen.

The spectral range of the camera used is between 3.7 µ m and 4.8 µm. The opening time is 10 ms and the frequency of collection of 10 or 100 Hz. A target of 50 mm focal length makes it possible to obtain a spatial resolution of 0.12 µm per pixel.

Test measure. The specimen was tested at ambient temperature (20°C) using piezoelectric fatigue machine (20 kHz) with a stress cyclic rate of R=-1.

Results and discussion

Mechanical results. The results of the tests in ultrasonic fatigue tests are shown in Fig 5 and 6.

In the ultrasonic fatigue test, test loading can cause an increase of the temperature of the specimen rapidly. The temperature evolution is related to the amplitude of cyclic load and loading rates. Temperature reflects the local plastic deformation of alloy; it can affect the fatigue life of specimen. So it is necessary to use a strong cooling air to cool the specimen in order to reduce the increase of the specimen temperature. To avoid a large increase of temperature at high stress amplitude, the loading is controlled step by step.

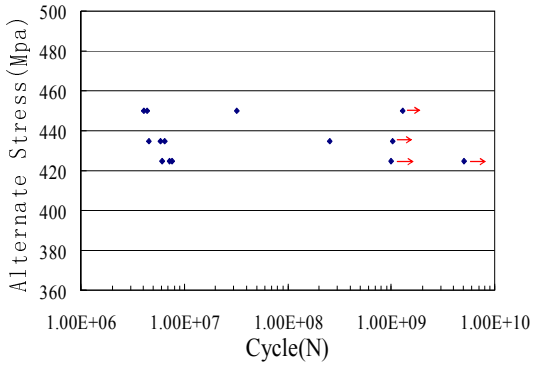

Fig.5 SN curve for R=0.01

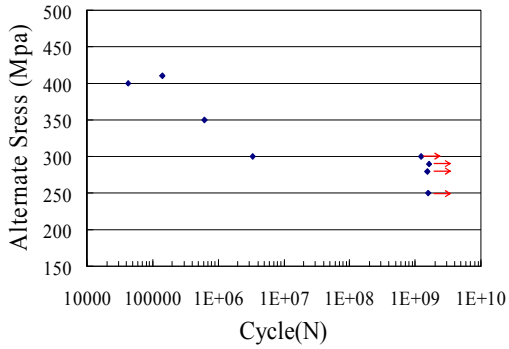

Fig. 6 SN curve for R=0.1

Thermal result. Self-heating temperature change of specimen during ultrasonic fatigue process is measured by infrared imaging system.

The test was conducted with amplitude of forced to 335MPa. During this test the rupture occurred after 8.37×10^7 cycles. Fig 7 shows the evolution of the maximum temperature at the surface of the specimen at the time of the rupture. There is then a dramatic rise of the temperature just before the break. The thermo-graphics of Fig 7B shows the temperature fields on the surface of the specimen at different moments represented in Fig 7A just before the break. It was found that the temperature is highly heterogeneous and that the temperature increase is much localized.

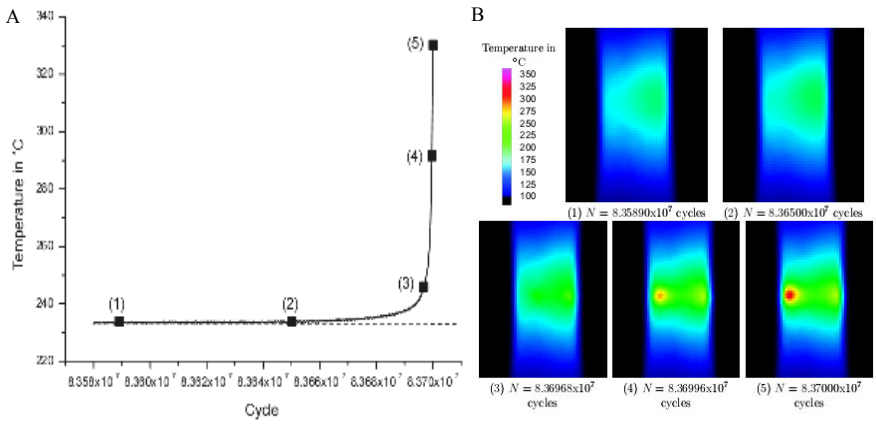

Fig.7 A) Temperature Evolution of the Specimen Surface just before Fracture, B) Temperature Fields on the Specimen Surface just before the Fracture ($\Delta\sigma$ = 335MPa, N = 8.37×10^7 cycles)

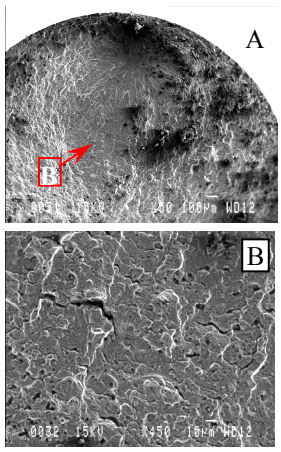

Fig.8 Fractography of Specimen N_f=3.19E+07, R=0.1, Fish eye

The number of cycles at the initiation Ni of fracture is given by point (1). It is 8.3589×10^7 cycles, whereas the number of cycles at fracture N_f is 8.37×10^7 cycles. The ratio Ni over N_f is 0.9987, that means 99.87% (for $N > 10^7$) of the total life is devoted to the initiation of the fracture.

Fractography

Observation of the fracture surface was made using a binocular and scanning electronic microscope (SEM).

Observation of the fracture surface shows a typical mechanism of initiation. Below 5×10^6cycles, the initiation of the crack is at the surface of the specimen. Beyond 5×10^6 cycles, the initiation is at the interior (Fig 8 and Fig 9). In this case, initiation is related to inclusion size. The direction of the red arrow in the fractography is the initiation of fatigue crack.

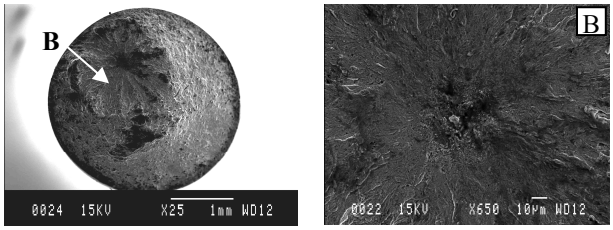

Fig. 9 Fractography of Specimen - N_f=2.53E+08, R=0.1, Fish Eye

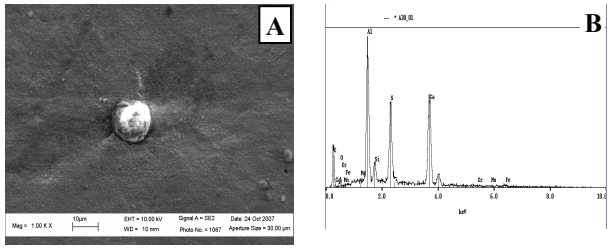

Fig. 10 A) An inclusion of specimen located beneath the surface, B) X-ray of the inclusion of Specimen

The specimen A30 used for thermal recording, the initiation is an inclusion located beneath the surface (Fig.10A), X-ray analysis (Fig.10B) shows that it is mixed inclusions (the larger inclusion) which are responsible of initiation. In the fish eye we can see striation (Fig.8A) and around fish eye, secondary cracks (Fig.9B).

Conclusion

a) The SN curve is very flat from 10^6 to 10^9 cycles but this steel can fail up to 10^9 cycles.
b) When strong cooling during the test is operated, beyond 10^6 cycles heating dissipation is negligible.
c) Beyond 5×10^6 cycles the initiation is located beneath the surface, on the larger inclusions.
d) 99.87% (for $N > 10^7$ and R=-1) of the total life is devoted to the initiation of the fracture.
e) If the screw hole of specimens were too long, it would made large scatter of test results.

References

[1] C.Bathias, P.Paris: *Gigacycle Fatigue in Mechanical Practice* (Marcel Dekker Inc. 2004, ISBN 0-8247-2313-9. DK3165)

[2] C.BATHIAS, ASTM STP, 2002. 1239:1411-1123

[3] Wang Q Y, C.BATHIAS, et al. International Journal of Fatigue 24 (2002)1260-1274

[4] Emin Bayraktar, et al., International Journal of Fatigue 28 (2006) 1590–1602

[5] Wang Q Y, Berafd J Y, Dubarre A, et al. Fatigue Fract. Eng. Mater. Struct., 1999, 22: 667~672

[6] Danninger H., Spoljaric D., Weiss B., et al., Zeischrift Fuer Metallkunde, 1998,89:135-141

[7] Marines I., Dominguez G., and et al. International Journal of Fatigue 25 (2003) 1037-1046

[8] I.Marines, X.Bin, C.BATHIAS, Intenational Journal of Fatigue 25 (2003) 1101-1107

[9] N. Ranc, D. Wagner, P.C. Paris, Acta Materialia 56 (2008) 4012 – 4021

[10] XUE Hongqian, TAO Hua, C.BATHIAS, ACTA AERONAUTICA ET ASTRONAUTICA SINICA, 2004, 25(4):425-428 (in Chinese)